

# Theory of noiseless phase-mixing amplification in a cavity optomechanical system

C. F. Ockeloen-Korppi,<sup>1</sup> T. T. Heikkilä,<sup>2</sup> M. A. Sillanpää,<sup>1</sup> and F. Massel<sup>2,\*</sup>

<sup>1</sup>*Department of Applied Physics, Aalto University, P.O. Box 15100, FI-00076 AALTO, Finland*

<sup>2</sup>*Department of Physics and Nanoscience Center, University of Jyväskylä,  
P.O. Box 35 (YFL), FI-40014 University of Jyväskylä, Finland*

The investigation of the ultimate limits imposed by quantum mechanics on amplification represents an important topic both on a fundamental level and from the perspective of potential applications. We propose here a novel setup for an optomechanical amplifier, constituted by a mechanical resonator dispersively coupled to an optomechanical cavity asymmetrically driven around both mechanical sidebands. We show that, on general grounds, the present amplifier operates in a novel regime— which we here call phase-mixing amplification. At the same time, for a suitable choice of parameters, the amplifier proposed here operates as a phase-sensitive amplifier. We show that both configurations allow amplification with an added noise below the quantum limit of (phase-insensitive) amplification in a parameter range compatible with current experiments in microwave circuit optomechanics.

The amplification of a signal constitutes one of the fundamental technical aspects of the modality through which modern information and communication technology operates, potentially paving the way towards the full technological exploitation of quantum mechanics [1]. At the same time it also represents a fundamental tool in the exploration of the properties of the world around us: with implications ranging from the exploration of quantum-mechanical properties of macroscopic objects [2] to the detection of gravitational waves [3]. In this context, it is thus relevant both from a conceptual and the applied point of view to investigate the boundaries imposed on the amplification of a signal, e.g. what kind of input we can effectively amplify and what are the properties of the output given a specific amplification setup.

In the context of quantum physics, a general result about the limits of amplification was derived by Haus [4] and Caves [5], stating that an amplifier, in order for its behaviour to be consistent with quantum mechanics, must add a minimum amount of noise, effectively preventing the possibility of cloning a quantum state [6]. In particular, if both quadratures of the input signal are amplified by the same amount, the minimum added noise corresponds to, in the large-gain limit, to half a quantum. Below, we refer to this limit as the amplification quantum limit (AQL) for phase-insensitive amplifiers. In the recent past, a lot of experimental and theoretical effort has been devoted to the amplification of quantum signals close to the quantum limit, in particular in the context of circuit quantum electrodynamics [7–9], and in optomechanical setups [10–14].

From the theoretical point of view, two possible alternatives have been contemplated to circumvent this limitation. One relies on the concept of “nondeterministic noiseless linear amplification” [15], according to which, with a probability of success  $p$ , it is possible to improve the signal-to-noise ratio beyond the AQL, with the limiting case of  $p = 0$  to attain noiseless amplification. The

second idea, dating back to Haus and Caves’ work, consists in considering a phase-sensitive amplifier, for which, at the expenses of increased fluctuations in one quadrature, it is possible to reduce the fluctuations in the other below the AQL imposed on phase-preserving linear amplifiers.

In this article, we elaborate on the second idea and we report how it is possible to reach below-AQL amplification in an optomechanical device suitably driven by two strong pumping tones. The conceptual relevance of such a device lies in the fact that it allows a faithful amplification on the level of single quanta, thus representing an ideal candidate in quantum-information processing applications, and in the detection of ultraweak signals. The present amplifier design possesses other advantages with respect to previous proposals: contrary to amplifiers based on Josephson junctions (see e.g. [7–9, 16]) whose inputs have relatively small dynamic range, the current amplifier works with comparably large inputs; compared to the optomechanical design proposed in [10] the bandwidth is orders of magnitude larger, making this device, on one hand a pivotal demonstration of how laws of quantum mechanics shape the properties of amplifiers, and, on the other, a device of unprecedented power and versatility whose design simplicity make it a perfect candidate for large-scale technological applications.

Furthermore, we show how the device proposed here can operate in a previously unreported regime: the analysis of multimode amplifiers has typically focused on a regime for which each output quadrature solely depends on a specific input quadrature (on top of the added noise) leading to the definition of phase-preserving, phase-conjugating and phase-sensitive amplification. Here we discuss how a more general scenario, in which either output quadrature can depend on both input quadratures.

## I. PHASE-MIXING AMPLIFICATION

The most general example of multimode linear amplifier can be described by the following input/output

\* francesco.p.massel@jyu.fi

relations [17]

$$a_{o\omega} = A_\omega a_{in\omega} + B_\omega a_{in-\omega}^\dagger + \mathcal{F}_{in\omega}, \quad (1)$$

where  $a_{in\omega}$ ,  $a_{out\omega}$  and  $\mathcal{F}_{in\omega}$  represent the operators associated with the input, output and added noise fields respectively [18]. As discussed in [5], Eq. (1) has to be intended as referred to a specific carrier frequency  $\omega_c$ , with respect to which the frequency  $\omega$ , and thus the quadratures, are defined (see appendix A).

We can write Eq. (1) in terms of input  $X_\omega^{1,2}$  and output  $Y_\omega^{1,2}$  quadratures as

$$Y_\omega^\theta = [A_{11}(\omega) \cos \theta - iA_{21}(\omega) \sin \theta] X_\omega^1 + [iA_{12}(\omega) \cos \theta + A_{22}(\omega) \sin \theta] X_\omega^2 + \mathcal{F}_\omega^\theta, \quad (2)$$

where

$$\begin{aligned} A_{11}(\omega) &= [(A_\omega + \bar{A}_\omega) + (B_\omega + \bar{B}_\omega)] / 2 \\ A_{12}(\omega) &= [(A_\omega - \bar{A}_\omega) - (B_\omega - \bar{B}_\omega)] / 2, \\ A_{21}(\omega) &= [(A_\omega - \bar{A}_\omega) + (B_\omega - \bar{B}_\omega)] / 2 \\ A_{22}(\omega) &= [(A_\omega + \bar{A}_\omega) - (B_\omega + \bar{B}_\omega)] / 2 \end{aligned} \quad (3)$$

with  $X_\omega^1 = a_{in-\omega}^\dagger + a_{in\omega}$ ,  $X_\omega^2 = i(a_{in-\omega}^\dagger - a_{in\omega})$ ,  $Y_\omega^\theta = (a_{in-\omega}^\dagger e^{i\theta} + a_{in\omega} e^{-i\theta})$ ,  $\mathcal{F}_\omega^\theta = (\mathcal{F}_{in-\omega}^\dagger e^{i\theta} + \mathcal{F}_{in\omega} e^{-i\theta})$ , and  $\bar{A}_\omega, \bar{B}_\omega = A_{-\omega}^*, B_{-\omega}^*$ . The phase  $\theta$  represents a controllable parameter, related to the homodyne detection scheme characterising phase-sensitive measurements both in the optical and in the microwave regime [19].

Defining  $Y_1 = Y_\omega^{\pi/2}$  and  $Y_2 = Y_\omega^0$ , we can write Eq. (2) in matrix form

$$\mathbf{Y} = \mathbf{A}\mathbf{X} + \mathcal{F} \quad (4)$$

with  $\mathbf{A} = [A_{11}, iA_{12}; -iA_{21}, A_{22}]$ ,  $\mathbf{Y} = [Y_1, Y_2]^T$ ,  $\mathbf{X} = [X_1, X_2]^T$ ,  $\mathcal{F} = [\mathcal{F}_1, \mathcal{F}_2]^T$ .

Equation (4) constitutes a generalisation of the analysis performed by Caves in the sense that we do not constrain the coefficients of Eq. (1) (and the corresponding equation for  $a_{o-\omega}^\dagger$ ) to obey the relation  $A_{-\omega}^* = A_\omega$ ,  $B_{-\omega}^* = B_\omega$ , as in the case discussed by Caves for multimode phase-sensitive amplifiers (see discussion before Eqs. 4.40 in ref. [5]), for which  $A_{12}$  and  $A_{21}$  would be identically zero.

In order to characterise the deviation from the case of multimode phase-sensitive amplification, we write the coefficients  $A_\omega$  and  $B_\omega$  in terms of their symmetric and antisymmetric frequency components

$$\begin{aligned} A_\omega &= A_{\Sigma\omega} + A_{\Delta\omega} \\ B_\omega &= B_{\Sigma\omega} + B_{\Delta\omega}, \end{aligned} \quad (5)$$

where  $A_{\Sigma\omega} = (A_\omega + A_{-\omega})/2$ ,  $A_{\Delta\omega} = (A_\omega - A_{-\omega})/2$  and analogously for  $B$ . In addition we exploit the gauge freedom for the input ( $a_{i\omega} \rightarrow a_{i\omega} \exp[i\phi_{i\omega}]$ ) and output fields ( $a_{o\omega} \rightarrow a_{o\omega} \exp[i\phi_{o\omega}]$ ) imposing that

$$\begin{aligned} \phi_{\Sigma\omega}^A &= \phi_{o\omega} - \phi_{i\omega} \\ \phi_{\Sigma\omega}^B &= \phi_{o\omega} - \phi_{i-\omega} = \phi_{o\omega} + \phi_{i\omega} \end{aligned} \quad (6)$$

where  $\phi_{\Sigma\omega}^A = \text{Arg}[A_{\Sigma\omega}]$ ,  $\phi_{\Sigma\omega}^B = \text{Arg}[B_{\Sigma\omega}]$ . We can write the equations of motion in a rotated frame, for which

$$\mathbf{Y} = \tilde{\mathbf{A}}\mathbf{X} \quad (7)$$

where

$$\begin{aligned} \tilde{A}_{11} &= |A_{\Sigma\omega}| + |B_{\Sigma\omega}| + i(|A_{\Delta\omega}| \cos \phi_1 + |B_{\Delta\omega}| \cos \phi_2) \\ \tilde{A}_{12} &= i(|B_{\Delta\omega}| \cos \phi_2 - |A_{\Delta\omega}| \cos \phi_1) \\ \tilde{A}_{21} &= i(|A_{\Delta\omega}| \cos \phi_1 + |B_{\Delta\omega}| \cos \phi_2) \\ \tilde{A}_{22} &= |A_{\Sigma\omega}| - |B_{\Sigma\omega}| + i(|A_{\Delta\omega}| \sin \phi_1 - |B_{\Delta\omega}| \sin \phi_2) \end{aligned} \quad (8)$$

with  $\phi_1 = \text{Arg}[A_{\Delta\omega}] - \text{Arg}[A_{\Sigma\omega}]$  and  $\phi_2 = \text{Arg}[B_{\Delta\omega}] - \text{Arg}[B_{\Sigma\omega}]$ . We note that, if  $A_{\Delta\omega} = B_{\Delta\omega} = 0$ , Eq. (8) corresponds to the usual input/output relation for a phase sensitive amplifier in the preferred quadratures.

In terms of algebraic properties, the possibility of diagonalising the matrix  $\mathbf{A}$  through a phase rotation of the input and output fields, corresponding to a rotation of the quadratures  $\mathbf{X} \rightarrow R_X \mathbf{X}$ ,  $\mathbf{Y} \rightarrow R_Y \mathbf{Y}$  is equivalent to the statement that for each real matrix  $\mathbf{M}$  there exists the singular value decomposition (SVD)

$$\mathbf{M} = \mathbf{U}\mathbf{D}\mathbf{V}^\dagger \quad (9)$$

where  $\mathbf{D}$  is a diagonal matrix and  $\mathbf{U}$  and  $\mathbf{V}$  are orthogonal matrices. However, if  $\mathbf{M}$  is a complex matrix, the SVD is possible only in terms of unitary matrices. Since a unitary transformation does not necessarily map quadrature operators to quadrature operators –the most prominent example being the mapping between  $a$ ,  $a^\dagger$  and (normalised) quadrature operators– we are led to conclude that, in general, not all matrices describing linear amplifiers can be put in a preferred quadrature form: more specifically due to the residual gauge freedom in the definition of input and output phases, the only transformations allowed are those defined by orthogonal matrices modulo an overall complex phase factor. We designate the regime for which it is not possible to cast the input-output relations for the field quadratures as phase-mixing amplification (PMA).

In addition, from the expression of the matrix elements given in Eq. (8), we note that  $\tilde{\mathbf{A}}$  is a diagonal matrix for  $\omega = 0$  and thus we recover the usual input/output expressions for a narrowband phase-sensitive linear amplifier

$$\begin{aligned} Y_1 &= A_{11}X_1 + \mathcal{F}_1 \\ Y_2 &= A_{22}X_2 + \mathcal{F}_2. \end{aligned} \quad (10)$$

This shows that PMA devices are intrinsically multimode amplifiers.

While we elaborate more about the noise analysis in the specific case of the optomechanical PMA, we note here that its analysis is somewhat complicated by the fact that the output in each quadrature depends on both

input quadratures. In general, we can write the output power spectrum as

$$S_Y^\theta = O_1^\theta S_1 + O_2^\theta S_2 + S_F^\theta \quad (11)$$

where  $S_Y^\theta = \frac{1}{4} (\langle Y_{-\omega}^\theta Y_\omega^\theta \rangle - 1)$ , and analogously for the input and noise spectra. From Eqs. (3, 4), we obtain

$$\begin{aligned} O_1^\theta &= \left[ |A_{11}|^2 \cos^2 \theta + |A_{21}|^2 \sin^2 \theta \right] \\ &\quad + \sin 2\theta |A_{11} A_{21}| \sin [\phi_{21} - \phi_{11}] \\ O_2^\theta &= \left[ |A_{22}|^2 \sin^2 \theta + |A_{12}|^2 \cos^2 \theta \right] \\ &\quad - \sin 2\theta |A_{22} A_{11}| \sin [\phi_{12} - \phi_{22}] \end{aligned} \quad (12)$$

with  $\phi_{ij} = \text{Arg}[A_{ij}]$ . In order to simplify our analysis, we will consider here an input for which  $S_1 = S_2$  (i.e. we exclude from our noise analysis the possibility of a squeezed input state) and therefore define the PMA power gain as

$$|\mathcal{G}^\theta|^2 = O_1^\theta + O_2^\theta. \quad (13)$$

This allows us to evaluate the added noise as referred to the input as

$$S_X^\theta = \frac{S_Y^\theta}{|\mathcal{G}^\theta|^2} \Big|_{S_1, S_2=0} = \frac{S_Y^\theta}{O_1^\theta + O_2^\theta} \Big|_{S_1, S_2=0}. \quad (14)$$

## II. OPTOMECHANICAL PMA

The setup considered to demonstrate PMA is represented by the prototypical, and arguably most simple, optomechanical cavity system, consisting of an electromagnetic (optical or microwave) cavity with resonant frequency  $\omega_c$  dispersively coupled to a mechanical oscillator whose resonance frequency is given by  $\omega_m$  (see e.g. [20]).

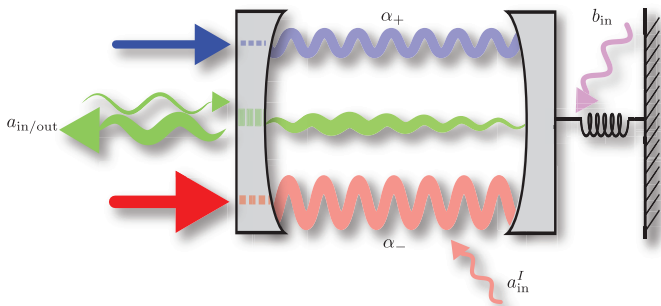


FIG. 1. Schematic representation of the setup discussed here. The cavity is driven by two tones at frequencies and intensities  $\omega_+$ ,  $\alpha_+$  (blue in the figure) and  $\omega_-$ ,  $\alpha_-$ , respectively (in red). In the figure we also indicate the input and output signals ( $a_{in}$ ,  $a_{out}$ ), and the internal and mechanical noise ( $a_{in}^I$  and  $b_{in}$ ).

The Hamiltonian of the system can be written as

$$H = \omega_c a^\dagger a + \omega_m b^\dagger b + g_0 a^\dagger (b^\dagger + b), \quad (15)$$

where  $a$  ( $a^\dagger$ ) and  $b$  ( $b^\dagger$ ) represent the raising (lowering) operators associated with the electromagnetic cavity field and the mechanical oscillator, respectively, and  $g_0$  is the single-photon optomechanical coupling strength. In addition to its internal dynamics, the system is coupled to an environment, which provides the possibility of driving and probing the system and, at the same time, represents a source for noise and dissipation, both for the mechanics and the cavity. Furthermore, we describe the noise/dissipation properties of the mechanical resonator through the coupling with a (phononic) thermal reservoir with average population  $n_m$ , and define a characteristic linewidth  $\gamma$ . An analogous assumption is adopted for the cavity. In this case, however, we consider a coupling to two different baths: the external bath (characterized by the linewidth  $\kappa_e$ ) providing both input signal and input noise, and an internal bath (linewidth  $\kappa_i$ ), associated with the internal losses of the cavity and whose population is given by  $n_c^I$ . Concerning the driving of the system,

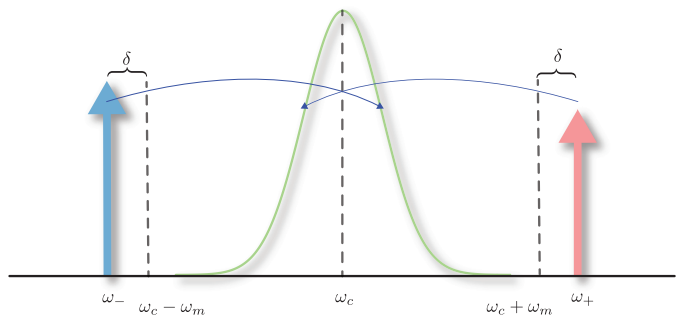


FIG. 2. Schematic representation of the pump intensities and frequencies with respect to the cavity frequency and linewidth. The mechanics-mediated scattering of pump photons scattered from the cavity around the cavity frequency resonance  $\omega_c$ .

we assume that the cavity is driven by two strong pumps of amplitude  $\alpha_+$  and  $\alpha_-$ , which are detuned with respect to the cavity resonant frequency  $\omega_c$ , by  $\omega_+ - \omega_c = \omega_m + \delta$  and  $\omega_- - \omega_c = -\omega_m - \delta$ , respectively (Fig. 2). A related two-tone setup has been previously considered in the context of backaction evading (BAE) measurements of the mechanical oscillator position [21–24], and in the generation of mechanical squeezing [25–27]. In both cases the frequencies of the driving tones were considered to fulfil the relation  $\omega_\pm = \omega_c \pm \omega_m$ . For equal pump amplitudes ( $\alpha_+ = \alpha_-$ ) this leads to the BAE detection of the mechanical oscillator position, and for  $\alpha_+ \neq \alpha_-$  to the squeezing of the mechanics below the standard quantum limit, defined as the uncertainty associated with the ground state of the mechanical oscillator.

In the presence of two strong driving tones, we can follow a standard approach and linearise the Hamiltonian given in Eq. (15). Neglecting fast oscillating terms (rotating-wave approximation) and moving to a frame rotating at  $\omega_c$  and  $\omega_m - \delta$  for the cavity and the mechanical

field, respectively, we can write it as

$$H = \delta b^\dagger b + G_+ a^\dagger b^\dagger + G_- a^\dagger b + h.c.. \quad (16)$$

where  $G_\pm = g_0 \alpha_\pm$ .

The solution of the equations of motion becomes simple after expressing Eq. (16) in terms of Bogoliubov modes for the cavity field

$$H = \delta b^\dagger b + G_{BG} (\alpha^\dagger b + \alpha b^\dagger), \quad (17)$$

where  $\alpha = u a + v a^\dagger$ ,  $G_{BG} = (G_-^2 - G_+^2)^{1/2}$ ,  $u = G_-/G_{BG}$ ,  $v = G_+/G_{BG}$ . The beam-splitter term  $G_{BG} (\alpha^\dagger b + \alpha b^\dagger)$  in Eq. (17) points towards the cooling of the mechanical motion to the temperature of the Bogoliubov cavity mode. As we show below, this entails the amplification of the unrotated cavity mode  $a$ .

From Eq. (17) we can determine the following quantum Langevin equations in the frequency domain for  $\alpha$  and  $b$

$$\begin{aligned} -i\omega\alpha_\omega &= -iG_{BG}b_\omega - \frac{\kappa}{2}\alpha_\omega + \sqrt{\kappa_e}\alpha_{in\omega} + \sqrt{\kappa_i}\alpha_{in\omega}^I \\ -i\omega b_\omega &= -i\delta b_\omega + iG_{BG}\alpha_\omega - \frac{\gamma}{2}b_\omega + \sqrt{\gamma}b_{in\omega}. \end{aligned} \quad (18)$$

Eliminating the mechanical degrees of freedom from Eq. (18), considering the usual input-output relation  $\alpha_{out\omega} + \alpha_{in\omega} = \sqrt{\kappa}\alpha_\omega$ , and transforming back to  $a_\omega$ , we can obtain an input/output relation for the output field  $a_{out\omega}$  (see Appendix B)

$$\begin{aligned} a_{out\omega} &= A_\omega a_{in\omega} + B_\omega a_{in-\omega}^\dagger + A_{I-\omega} a_{in\omega}^I + B_{I\omega} a_{in-\omega}^{I\dagger} \\ &\quad + C_\omega b_{in\omega} + D_\omega b_{in-\omega}^\dagger. \end{aligned} \quad (19)$$

The coefficients in Eq. (19) are given by

$$\begin{aligned} A_\omega &= \kappa_e (u^2 \chi_c^{\text{eff}} - v^2 \bar{\chi}_c^{\text{eff}}) - 1 \\ A_{I\omega} &= \sqrt{\kappa_i \kappa_e} (u^2 \chi_c^{\text{eff}} - v^2 \bar{\chi}_c^{\text{eff}}) \\ B_\omega &= uv \kappa_e (\chi_c^{\text{eff}} - \bar{\chi}_c^{\text{eff}}) \\ B_{I\omega} &= uv \sqrt{\kappa_i \kappa_e} (\chi_c^{\text{eff}} - \bar{\chi}_c^{\text{eff}}) \\ C_\omega &= -iG_- \sqrt{\gamma \kappa_e} \chi_c^{\text{eff}} \chi_m \\ D_\omega &= iG_+ \sqrt{\gamma \kappa_e} \chi_c^{\text{eff}} \bar{\chi}_m \end{aligned} \quad (20)$$

with  $\bar{\chi} = \chi^*(\omega \rightarrow -\omega)$ ,  $\chi = \chi_c^{\text{eff}}$ ,  $\chi_m$ , and

$$\begin{aligned} \chi_c^{\text{eff}} &= [\kappa/2 - i\omega + G_{BG}^2 \chi_m]^{-1}, \\ \chi_m &= [\gamma/2 - i(\omega - \delta)]^{-1}. \end{aligned} \quad (21)$$

Equations (20,21) allow us to identify, for the optomechanical case, the parameters defined in Eq. (4). More specifically, the definitions given in (20) allow us to evaluate  $O_1^\theta$ ,  $O_2^\theta$ , and  $S_F$ , therefore characterising the PMA properties of the system. In Fig. 3 we characterise the phase-mixing properties of the amplifier. In particular it is possible to see that, at the maximum-gain frequency  $\omega_{max}$  (see Eq. (23) below) we have that

$|\mathcal{G}^{\pi/2}(\omega)|^2 \simeq O_1^{\pi/2}$  (Fig. 3(b)) and  $|\mathcal{G}^0(\omega)|^2 \simeq O_2^0$  (Fig. 3(c)). From Eqs. (12,13), this implies the coefficients  $A_{11}$  and  $A_{22}$  are negligible with respect to the diagonal terms, and therefore allow us to describe the device as a phase sensitive amplifier,

$$\begin{aligned} Y_1 &\simeq A_{12} X_2 + \mathcal{F}_2 \\ Y_2 &\simeq A_{21} X_1 + \mathcal{F}_1. \end{aligned} \quad (22)$$

If we are in a sideband resolved-like regime, i.e. if the two peaks depicted in Fig. 3 can be approximately treated as separate peaks for  $\kappa_e \simeq \kappa$  and  $\gamma \simeq 0$ , it is possible to express the gain in terms of a Lorentzian centered around  $\omega_{max}$  and linewidth  $\gamma_{eff}$ , where

$$\begin{aligned} \omega_{max} &= \pm \delta \left[ 1 + \frac{G_{BG}^2}{\kappa^2/4 + \delta^2} \right] \\ \gamma_{eff} &= \frac{G_{BG}^2 \kappa}{\kappa^2/4 + \delta^2}. \end{aligned} \quad (23)$$

These expressions are hence valid for  $\omega_{max} \gg \gamma_{eff}$ . Crucially, for the description of this optomechanical system in terms of PMA, away from the resonance defined by Eq. (23) the mixing coefficients  $A_{11}$  and  $A_{22}$  start to play a significant role (see Fig. 3), and a real-valued SVD decomposition becomes, in general, not possible. In the limit  $G_{BG} \ll \delta$ ,  $\delta \ll \kappa$  the coefficients  $A_{ij}$  assume a particularly simple form

$$\begin{aligned} A_{21} &= -\frac{2/\kappa (G_- + G_+)^2}{\frac{\gamma_{eff}}{2} - i(\omega - \omega_{max})} \\ A_{12} &= -\frac{2/\kappa (G_- - G_+)^2}{\frac{\gamma_{eff}}{2} - i(\omega - \omega_{max})} \\ A_{11} = A_{22} &= \left[ 1 - \frac{2G_{BG}^2/\kappa}{\frac{\gamma_{eff}}{2} - i(\omega - \omega_{max})} \right]. \end{aligned} \quad (24)$$

Eqs. (23,24) allow us to evaluate an approximate expression for the gains at resonance ( $\omega = \omega_{max}$ )

$$\begin{aligned} |\mathcal{G}_1| &= (u + v)^2 \\ |\mathcal{G}_2| &= (u - v)^2 \end{aligned} \quad (25)$$

and therefore the value of the gain-bandwidth product

$$\mathcal{G}_1 \gamma_{eff} |_{\omega=\omega_{max}} = 16 \frac{G_+^2 G_-^2}{\kappa G_{BG}^2}. \quad (26)$$

Furthermore, given the definitions of  $u$  and  $v$ , which can be also expressed as  $u = \cosh \xi$ ,  $v = \sinh \xi$ , we can recover the condition

$$|\mathcal{G}_1 \mathcal{G}_2| = 1 \quad (27)$$

characterising a degenerate parametric amplifier, which can be considered as the ‘‘gold standard’’ of phase-sensitive amplifiers. Furthermore, it is clear from Eq. (24) that, in the limit discussed here, the frequency range

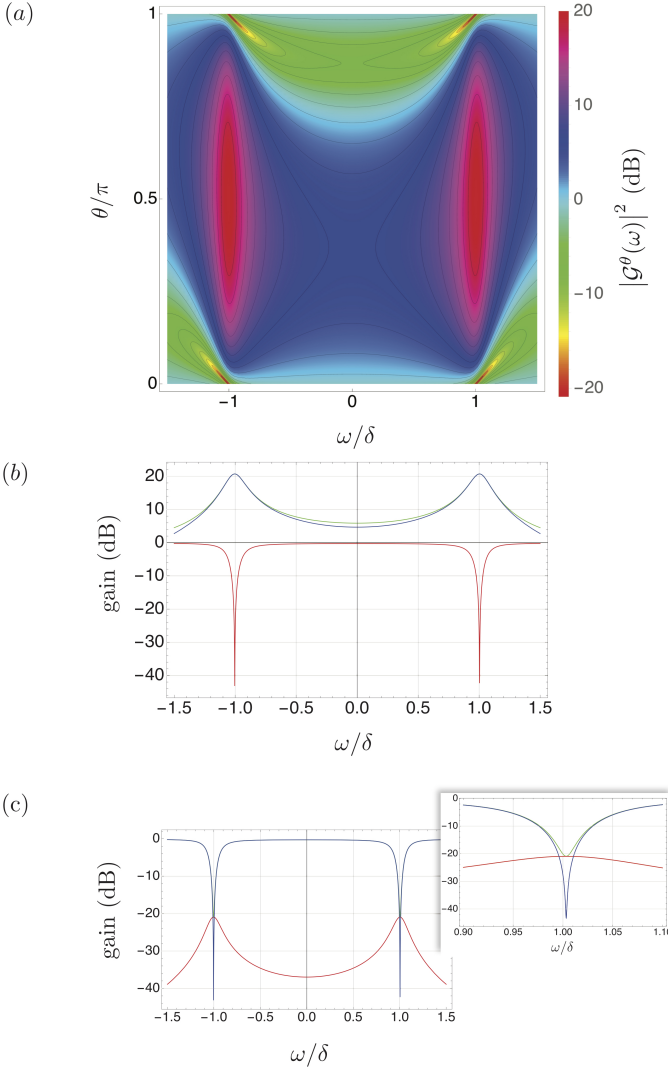


FIG. 3. (a) Gain for below-AQL amplification (see Eq. (35) below) as a function of  $\theta$  and  $\omega$ . Detail of the frequency dependence around  $\omega_{max}$  of  $|\mathcal{G}^\theta(\omega)|^2$  (green),  $O_1^\theta(\omega)$  (blue),  $O_2^\theta(\omega)$  (red), for  $\theta = \pi/2$  (b) and  $\theta = 0$  (c). Parameters:  $G_+ = 0.06$ ,  $G_- = 0.072$ ,  $\delta = 0.04$ ,  $\kappa_e = 0.99$ ,  $\gamma = 2 \cdot 10^{-5}$ , energies in units of the cavity linewidth  $\kappa$ . The frequency  $\omega = 0$  corresponds to the cavity resonant frequency.

around  $\omega_{max}$  for which the system can be characterised as a phase-sensitive amplifier is given by  $\gamma_{eff}$ .

In Fig. 4 we plot the gain  $|\mathcal{G}^\theta(\omega)|^2$  as a function of  $\theta$  for different values of  $\omega$ . The crucial feature of this plot is the  $\omega$ -dependence of the gain maximum. This dependence, which plays an important role in the determination of the noise properties of the system, can be ascribed to a finite value of  $A_{11}$  and  $A_{22}$ . From Eqs. (12,13), it is possible

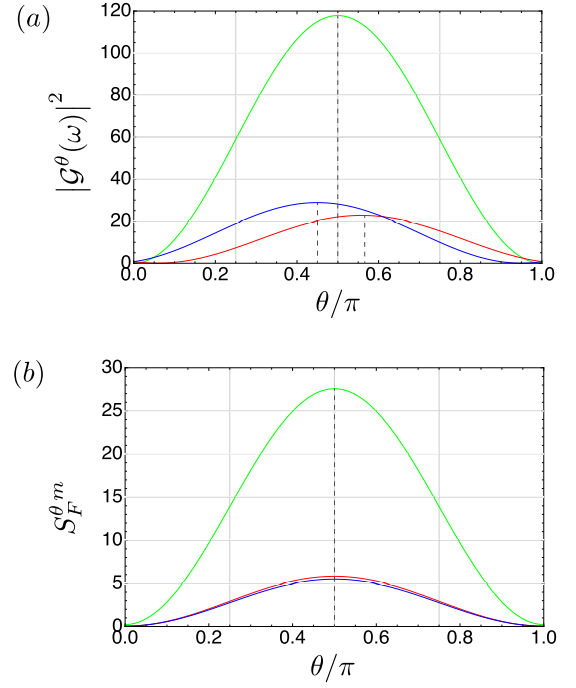


FIG. 4. (a) Gain  $|\mathcal{G}^\theta(\omega)|^2$  for the same parameters as in Fig. 3, for  $\omega = \omega_{max}$  (green),  $\omega = \omega_{max} - \gamma_{eff}$  (red),  $\omega = \omega_{max} + \gamma_{eff}$  (blue). The maximum point is at  $\theta = \pi/2$  for  $\omega = \omega_{max}$ , and shifted from this point for  $\omega = \omega_{max} \pm \gamma_{eff}$ . (b) Mechanical contribution to the added noise  $S_F^{\theta,m}$  for  $\omega = \omega_{max}$  (green),  $\omega = \omega_{max} - \gamma_{eff}$  (red),  $\omega = \omega_{max} + \gamma_{eff}$  (blue). In this case, the maximum point lies at  $\theta$  for all values of  $\omega$ .

to write  $|\mathcal{G}^\theta(\omega)|^2$  as

$$|\mathcal{G}^\theta(\omega)|^2 = |A_{11}(\omega)|^2 \cos^2 \theta + |A_{21}(\omega)|^2 \sin^2 \theta + s_{2\theta} |A_{11} A_{21}| s_{\Delta_1} + |A_{22}(\omega)|^2 \sin^2 \theta + |A_{12}(\omega)|^2 \cos^2 \theta - s_{2\theta} |A_{22} A_{12}| s_{\Delta_2}, \quad (28)$$

with  $s_{\Delta_1} = \sin(\phi_{21} - \phi_{11})$  and  $s_{\Delta_2} = \sin(\phi_{12} - \phi_{22})$ . Moreover, since  $|A_{12}| = |A_{21}|$ , we can write

$$|\mathcal{G}^\theta(\omega)|^2 = \mathcal{A}_s + \mathcal{A}_x + \mathcal{A}_\Delta \cos[2\theta + \phi] \quad (29)$$

with  $\mathcal{A}_{s,\Delta} = |A_{11}|^2 \pm |A_{22}|^2$ ,  $\mathcal{A}_x = |A_{12}|^2 = |A_{21}|^2$ ,  $\mathcal{A}_\phi = \sqrt{\mathcal{A}_x} (|A_{11}| s_{\Delta_1} - |A_{12}| s_{\Delta_2})$ ,  $\mathcal{A}_\Delta = \sqrt{\mathcal{A}_D^2 + \mathcal{A}_\phi^2}$ ,  $\phi = \arctan \frac{\mathcal{A}_\phi}{\mathcal{A}_D}$ . Eq. (29) the frequency-dependence of the maximum gain angle through the frequency dependence of the added phase factor  $\phi$ .

In order to show that away from  $\omega = \omega_{max}$  the amplifier cannot be described in terms of phase-sensitive amplification, we evaluate for the optomechanical case the frequency dependence of the phases  $\text{Arg}[\tilde{A}_{11}]$  and  $\text{Arg}[\tilde{A}_{22}]$ —note that  $\text{Arg}[\tilde{A}_{12}] = \text{Arg}[\tilde{A}_{21}] = \pm\pi/2$ , see Eq. (8). Since for  $\omega = 0$ ,  $\tilde{A}_{21} = \tilde{A}_{12} = 0$  and  $\tilde{A}_{11}, \tilde{A}_{22}$

are both real (see Fig. 5), the matrix  $\tilde{A}$  is, in this case, real, and therefore real-valued SVD, corresponding to a rotation to the preferred quadratures, is possible. Analogously, for  $\omega = \omega_{max}$  the phases of all four terms are equal, implying that, in this case the matrix  $\tilde{A}$  is proportional to a real matrix and thus, again it can be rotated to the preferred quadratures. For all other frequency val-

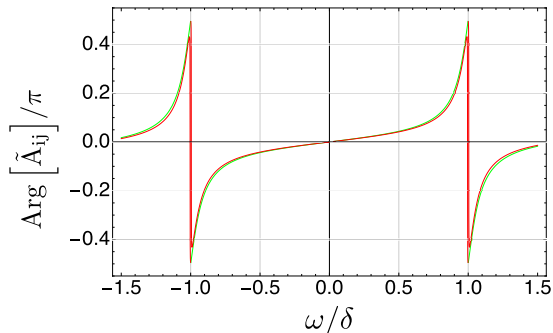


FIG. 5. Phase of  $\tilde{A}_{11}$  (green),  $\tilde{A}_{22}$  (red). For  $\omega = 0$  and  $\omega = \omega_{max}$  phase-sensitive amplification is possible, for other values of  $\omega$  the amplifier behaves as a phase-mixing device.

ues, since all terms of matrix  $\tilde{\mathbf{A}}$  are non-vanishing and possess different phases, real-valued SVD is not possible and thus a rotation to the preferred quadratures is not possible.

### III. NOISE PROPERTIES

We turn now to the discussion of the added noise properties of the amplifier, assuming that both the mechanical oscillator and the cavity field are subject to noise—below referred to as mechanical and internal noise (see Fig. 1). Otherwise stated, we assume that we can write the added noise as  $\mathcal{F}_\theta = \mathcal{F}_\theta^m + \mathcal{F}_\theta^I$ , where

$$\mathcal{F}_\theta^m = [A_{11}^m \cos \theta - iA_{21}^m \sin \theta] X_\omega^{1m} + [iA_{12}^m \cos \theta - iA_{22}^m \sin \theta] X_\omega^{2m} \quad (30)$$

where  $A_{ij}^m$ s are defined from Eq. (20), in analogy to the definitions given in Eq. (3) for the input signals and  $\mathcal{F}_\theta^I$  is obtained the same way by replacing the superscript  $m$  by  $I$  in Eq. (30). Focusing on the  $\omega = \omega_{max}$  resonance, with the same approximations as the ones used in the derivation of the gain coefficients, we have

$$A_{11}^m(\omega) = A_{12}^m(\omega) = -\frac{i\sqrt{\gamma\kappa_e}}{\kappa} \frac{G_- - G_+}{\frac{\gamma_{eff}}{2} - i(\omega - \omega_{max})}$$

$$A_{22}^m(\omega) = A_{21}^m(\omega) = -\frac{i\sqrt{\gamma\kappa_e}}{\kappa} \frac{G_- + G_+}{\frac{\gamma_{eff}}{2} - i(\omega - \omega_{max})}. \quad (31)$$

For the internal noise, with the same approximations considered for the calculation of the gain, we have

$$A_{21}^I = \frac{-2\kappa_i/\kappa^2 (G_- + G_+)^2}{\frac{\gamma_{eff}}{2} - i(\omega - \omega_{max})}$$

$$A_{12}^I = \frac{-2\kappa_i/\kappa^2 (G_- - G_+)^2}{\frac{\gamma_{eff}}{2} - i(\omega - \omega_{max})}$$

$$A_{11}^I = A_{22}^I = \frac{\kappa_i}{\kappa} \left[ 1 - \frac{2G_{BG}^2/\kappa}{\frac{\gamma_{eff}}{2} - i(\omega - \omega_{max})} \right] + \frac{\kappa_i}{\kappa}. \quad (32)$$

With the expressions given by Eq. (25), and excluding the possibility of squeezed noise, we can write the contribution to the added noise as

$$S_F^{\theta m} = 2 \left[ |A_{11}^m|^2 \cos^2 \theta + |A_{22}^m|^2 \sin^2 \theta \right] (2n_m + 1), \quad (33)$$

where  $n_m$  is the thermal population of the mechanical bath and analogously for the internal cavity noise.

Assuming that  $\kappa_i \ll \kappa$ , and  $n_c^I \ll N_m$  in the regime relevant for the experiment, corresponding to a cavity thermal occupation of less than one quantum and to a thermal bath for the mechanical resonator of a few hundreds quanta, the contribution from the mechanical noise is dominant. The approximate expressions given in Eq. (25), allow us to write the total added noise at  $\omega = \omega_{max}$  as

$$S_{add}^\theta = \frac{S_F^{\theta m} + S_F^{\theta I}}{|\mathcal{G}_\omega^\theta|^2}$$

$$\simeq \frac{\gamma\kappa \left[ (G_- + G_+)^2 \sin^2 \theta + (G_- - G_+)^2 \cos^2 \theta \right]}{2 \left[ (G_- + G_+)^4 \sin^2 \theta + (G_- - G_+)^4 \cos^2 \theta \right]} \cdot (2n_m + 1) \quad (34)$$

For  $G_- \gtrsim G_+$ , this expression allows establishing a condition under which the quantum limit for phase-insensitive amplification is overcome by the (phase-sensitive) optomechanical amplifier discussed here, namely

$$(G_- + G_+)^2 > \gamma\kappa(2n_m + 1) \implies S_{add}^\theta < 1/2 \quad (35)$$

for  $\theta \neq 0$ . On the other hand, even if the condition given by Eq. (35) is not fulfilled, it is still possible to “beat” the quantum limit in the PMA regime, reaching  $S_{add,m} < 1/2$  away from  $\omega = \omega_{max}$ . This relies on the different phase dependence of mechanical added noise and gain. Namely, the condition  $A_{11} \neq 0$  allows for a shift in the location of the maximum of  $\mathcal{G}_\omega^\theta$  as a function of  $\theta$ . Since this phase shift is absent for the added mechanical noise (see Fig. 4(b)), the presence of a  $A_{11} \neq 0$  term effectively allows for a relative shift of the phases for which gain and noise reach their maxima.

Stated otherwise, it is possible to reach amplification with noise properties below the quantum limit by shifting the input signal frequency away from  $\omega_{max}$ . In Figs. 6,7 we depict the added noise as a function of  $\omega$  and  $\theta$  for a value of the pump intensities leading to amplification



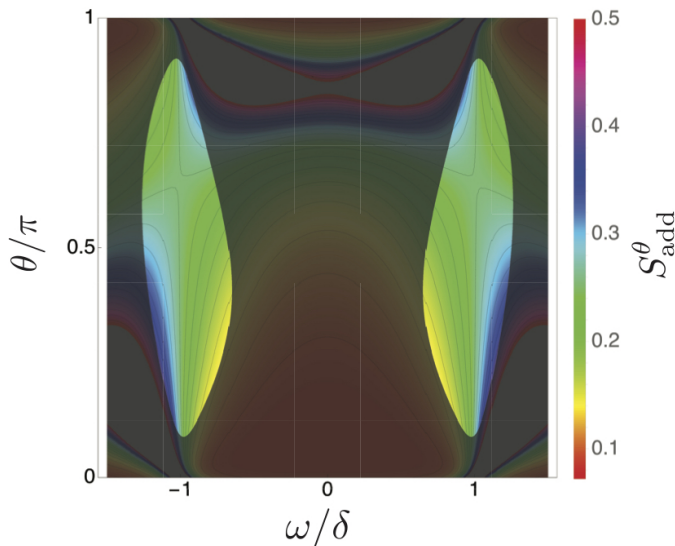


FIG. 6. Total added noise for a drive fulfilling the condition given in Eq. (35) ( $n_m = 200$ ,  $n_c^I = 0.1$  all other parameters as in Fig. 4). Grey areas correspond to regions with added noise larger than the AQL, as a guide to the eye, the light-coloured areas correspond to a gain larger than 10.

with noise properties below the AQL for  $\omega = \omega_{max}$ . In Fig. 7(b),(c) it is possible to see that shifting away from  $\omega = \omega_{max}$  leads to a reduction of the region for which  $S_{add}^\theta < 1/2$ .

In Figs. 8,9, where we plot the total added noise for a pump leading to amplification with noise properties above the AQL for  $\omega = \omega_{max}$ , the converse is true: shifting away from  $\omega = \omega_{max}$ , leads to the possibility of reaching below AQL amplification. This is a direct consequence of the different  $\theta$ -dependence of the gain  $\mathcal{G}^\theta(\omega)$  and the mechanical contribution to the added noise  $S_F^{\theta,m}$ .

#### IV. CONCLUSIONS

We have here demonstrated a novel regime of quantum signal amplification beyond the usual phase-insensitive/phase-sensitive amplification paradigm, which we call phase-mixing amplification. In addition, we have provided a specific example of phase-sensitive amplification in the context of optomechanics, demonstrating the possibility of below-AQL amplification and showing how the different phase dependence of gain and noise can increase the parameters range over which below-AQL amplification is possible.

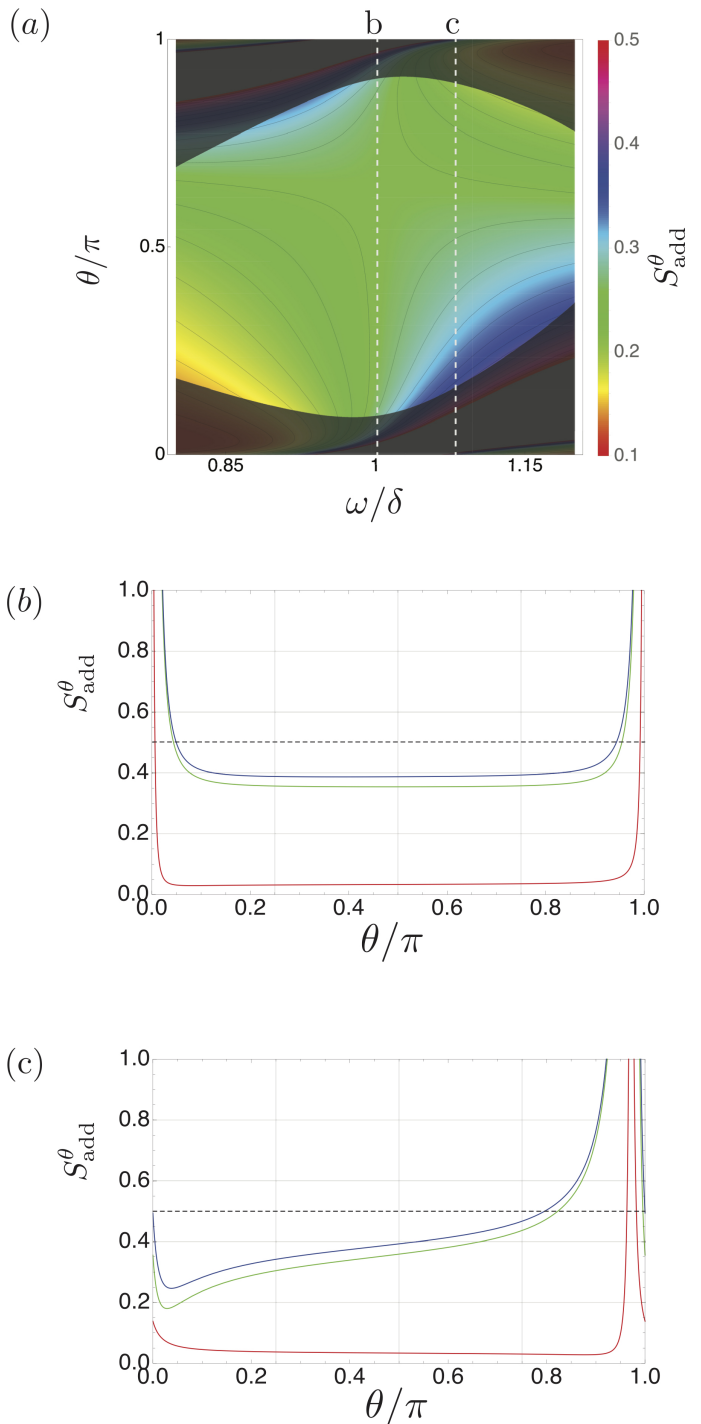


FIG. 7. (a) Zoom of figure 6 for  $\omega \simeq \delta$ , dashed lines correspond to the plots in (b) and (c). (b-c) Total (blue), mechanical (green), internal (red) added noise for the same drive as in Fig 6: (b) on resonance ( $\omega = \omega_{max}$ ), (c) off resonance ( $\omega = \omega_{max} + \gamma_{eff}$ ).

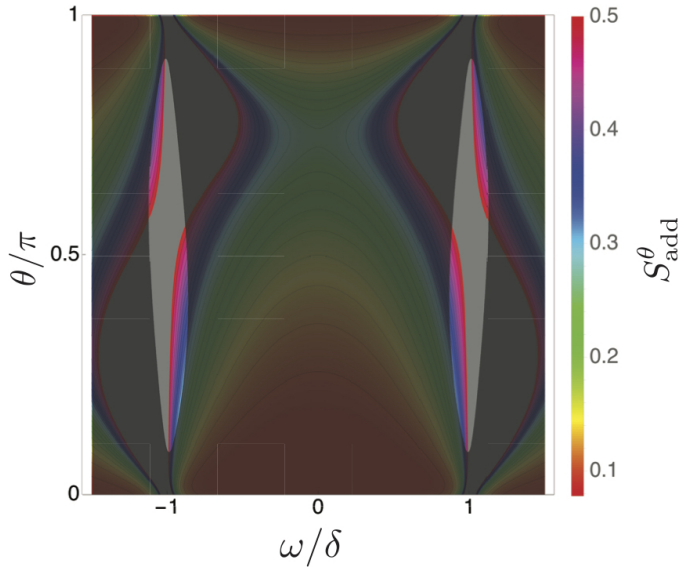


FIG. 8. Total added noise for a drive below  $\gamma\kappa(2n_m + 1)$  ( $G_+ = 0.04, G_- = 0.048$ , all other parameters as in the previous figures). Grey areas correspond to regions with added noise larger than the AQL

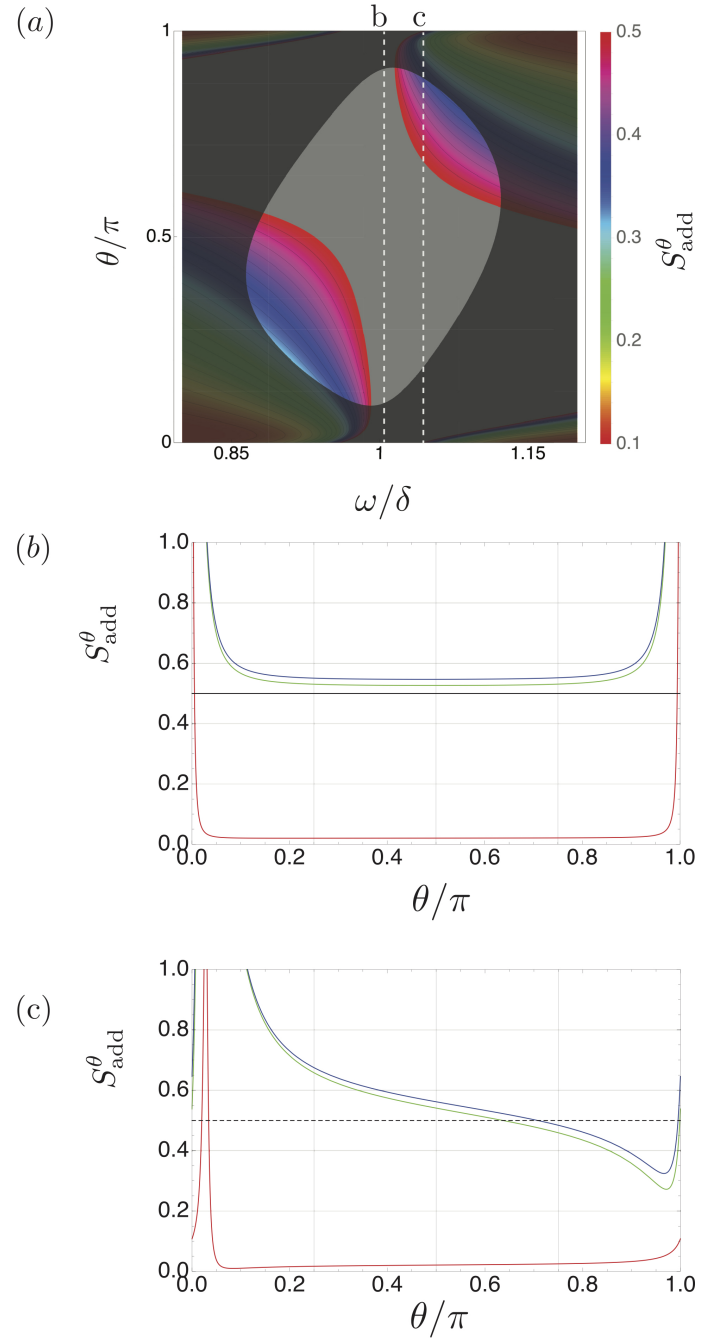


FIG. 9. (a) Zoom of figure 8 for  $\omega \simeq \delta$ , dashed lines correspond to the plots in (b) and (c). (b-c) Total (blue), mechanical (green), internal (red) added noise for the same drive as in Fig 8: (b) on resonance ( $\omega = \omega_{max}$ ), (c) off resonance ( $\omega = \omega_{max} + \gamma_{eff}$ ).



## Appendix A: PMA for a coherent field

In order to further clarify the concept of phase-mixing amplification, we provide a simple example of how a phase-mixing amplifier works for an input characterised by a coherent monochromatic signal defined around a carrier frequency  $\omega_0$  as

$$\langle \mathbf{E} \rangle \propto x_1(t) \cos \omega_0 t + x_2(t) \sin \omega_0 t \quad (\text{A1})$$

where  $x_1(t) \doteq \langle X_1 \rangle$ ,  $x_2(t) \doteq \langle X_2 \rangle$  represent the (slowly) time-varying expectation values of quadrature fields, defined with respect to the carrier frequency  $\omega_0$ . If we assume that

$$\begin{aligned} x_1(t) &= \Xi_1 \cos(\bar{\omega}t + \phi) \\ x_2(t) &= \Xi_2 \sin(\bar{\omega}t + \phi) \end{aligned} \quad (\text{A2})$$

or, analogously, in frequency domain

$$\begin{aligned} x_1(\omega) &= \Xi_1 [e^{-i\phi_1} \delta(\bar{\omega} - \omega) + e^{i\phi_1} \delta(\bar{\omega} + \omega)] \\ x_2(\omega) &= \Xi_2 [e^{-i\phi_2} \delta(\bar{\omega} - \omega) + e^{i\phi_2} \delta(\bar{\omega} + \omega)], \end{aligned} \quad (\text{A3})$$

(where we have set  $\phi_1 = \phi$  and  $\phi_2 = \phi - \pi/2$ ) and considering the I/O relations for the phase-mixing amplifier –Eqs. (4)– we can write the expression for the output field quadratures time dependence, defined around the carrier frequency  $\omega_0$  as for the input field, (neglecting the noise sources) as

$$\begin{aligned} y_\theta(t) &= \left\{ [A_{11}(\bar{\omega}) \cos \theta - iA_{21}(\bar{\omega}) \sin \theta] e^{-i(\bar{\omega}t + \phi_1)} + \right. \\ &\quad \left. [A_{11}(-\bar{\omega}) \cos \theta - iA_{21}(-\bar{\omega}) \sin \theta] e^{i(\bar{\omega}t + \phi_1)} \right\} \Xi_1 + \\ &\quad \left\{ [iA_{12}(\bar{\omega}) \cos \theta + A_{22}(\bar{\omega}) \sin \theta] e^{-i(\bar{\omega}t + \phi_2)} + \right. \\ &\quad \left. [iA_{12}(-\bar{\omega}) \cos \theta + A_{22}(-\bar{\omega}) \sin \theta] e^{i(\bar{\omega}t + \phi_2)} \right\} \Xi_2. \end{aligned} \quad (\text{A4})$$

Since  $A_{ij}(\bar{\omega}) = A_{ij}^*(-\bar{\omega})$ , Eq. (A4) can be written as

$$\begin{aligned} y_{\theta t} &= [ |A_{11}(\omega)| \cos \theta \cos(\bar{\omega}t + \bar{\phi}_{11}) \\ &\quad - |A_{21}(\omega)| \sin \theta \sin(\bar{\omega}t + \bar{\phi}_{21}) ] \Xi_1 + \\ &\quad [ |A_{22}(\omega)| \sin \theta \cos(\bar{\omega}t + \bar{\phi}_{22}) \\ &\quad + |A_{12}(\omega)| \cos \theta \sin(\bar{\omega}t + \bar{\phi}_{12}) ] \Xi_2, \end{aligned} \quad (\text{A5})$$

where we have defined  $\bar{\phi}_{ij} = \phi_j - \phi_{ij}$ . Eq. (A5) can be written also as

$$y_{\theta t} = [ \mathcal{A}_1 \cos(\bar{\omega}t + \bar{\phi}_1^\theta) \Xi_1 + \mathcal{A}_2 \sin(\bar{\omega}t + \bar{\phi}_2^\theta) \Xi_2 ] \quad (\text{A6})$$

having defined

$$\begin{aligned} \mathcal{A}_1 &= \sqrt{|A_{11} \cos \theta|^2 + |A_{21} \sin \theta|^2 + A_{11} A_{21} s_{2\theta} \sin(\bar{\phi}_{11} - \bar{\phi}_{21})} \\ \mathcal{A}_2 &= \sqrt{|A_{22} \sin \theta|^2 + |A_{12} \cos \theta|^2 - A_{12} A_{22} s_{2\theta} \sin(\bar{\phi}_{22} - \bar{\phi}_{12})} \end{aligned} \quad (\text{A7})$$

and

$$\begin{aligned} \bar{\phi}_1^\theta &= \arctan \frac{A_{11} \cos \theta \sin \bar{\phi}_{11} + A_{21} \sin \theta \cos \bar{\phi}_{21}}{A_{11} \cos \theta \cos \bar{\phi}_{11} - A_{21} \sin \theta \sin \bar{\phi}_{21}} \\ \bar{\phi}_2^\theta &= \arctan \frac{A_{12} \cos \theta \sin \bar{\phi}_{12} + A_{22} \sin \theta \cos \bar{\phi}_{22}}{A_{12} \cos \theta \cos \bar{\phi}_{12} - A_{22} \sin \theta \sin \bar{\phi}_{22}}. \end{aligned} \quad (\text{A8})$$

Finally, from Eq. (A8), it is possible to write

$$y_{\theta t} = \mathcal{A}_\theta \cos(\bar{\omega}t + \eta_\theta) \Xi \quad (\text{A9})$$

with

$$\mathcal{A}_\theta \Xi = \sqrt{\mathcal{A}_1^2 \Xi_1^2 + \mathcal{A}_2^2 \Xi_2^2 + 2\mathcal{A}_1 \mathcal{A}_2 \Xi_1 \Xi_2 \sin(\bar{\phi}_2 - \bar{\phi}_1)} \quad (\text{A10})$$

and

$$\eta_\theta = \arctan \left[ \frac{\mathcal{A}_1 \sin \bar{\phi}_1 - \mathcal{A}_2 \cos \bar{\phi}_2}{\mathcal{A}_1 \cos \bar{\phi}_1 - \mathcal{A}_2 \sin \bar{\phi}_2} \right]. \quad (\text{A11})$$

In the case of real coefficients  $A_{ij}$ , Eq. (A11) allows to evaluate the expression for the output quadratures  $y_1 \doteq y_{\theta=0}$ ,  $y_2 \doteq y_{\theta=\pi/2}$  as

$$\begin{aligned} y_{1t} &= \sqrt{A_{11}^2 \Xi_1^2 + A_{12}^2 \Xi_2^2} \cos(\bar{\omega}t + \phi) \\ y_{2t} &= \sqrt{A_{22}^2 \Xi_2^2 + A_{21}^2 \Xi_1^2} \sin(\bar{\omega}t + \phi) \end{aligned} \quad (\text{A12})$$

clearly showing how each output quadrature depends on the amplitude of both input quadratures.

The analysis performed above represents a simple example of how each output quadrature depends on both input quadratures, allowing thus to tailor the phase properties of the output signal with far reaching consequences, as we outline in the analysis of the specific optomechanical device proposed here.

## Appendix B: Derivation of the I/O EOMs

The mechanical degrees of freedom can be eliminated from Eq. (18), leading to the following equation for the Bogoliubov mode  $\alpha$

$$\begin{aligned} -i\omega \alpha_\omega &= G_{BG}^2 \chi_m \alpha_\omega - \frac{\kappa}{2} \alpha_\omega \\ &\quad + \sqrt{\kappa} \alpha_{in \omega} - iG_{BG} \chi_m \sqrt{\gamma} b_{in \omega} \end{aligned} \quad (\text{B1})$$

which can be solved to give

$$\alpha_\omega = \chi_c^{\text{eff}} \sqrt{\kappa} \tilde{\alpha}_{in \omega}. \quad (\text{B2})$$

where

$$\sqrt{\kappa} \tilde{\alpha}_{in \omega} = \sqrt{\kappa} \alpha_{in \omega} - iG_{BG} \chi_m \sqrt{\gamma} b_{in \omega}. \quad (\text{B3})$$

- 
- [1] A. A. Clerk, et al., *Rev. Mod. Phys.* **82**, 1155 (2010).
- [2] W. H. Zurek, *Phys Today* **44**, 36 (1991).
- [3] B. P. Abbott, et al., *Phys. Rev. Lett.* **116**, 061102 (2016).
- [4] H. A. Haus and J. Mullen, *Phys. Rev.* **128**, 2407 (1962).
- [5] C. M. Caves, *Phys. Rev. D* **26**, 1817 (1982).
- [6] W. K. Wootters and W. H. Zurek, *Nature* **299**, 802 (1982).
- [7] M. A. Castellanos-Beltran, et al., *Nat. Phys.* **4**, 929 (2008).
- [8] N. Bergeal, et al., *Nature* **465**, 64 (2010).
- [9] L. Zhong, et al., *New J Phys* **15**, 125013 (2013).
- [10] F. Massel, et al., *Nature* **480**, 351 (2011).
- [11] A. Metelmann and A. A. Clerk, *Phys. Rev. Lett.* **112**, 133904 (2014).
- [12] A. Metelmann and A. A. Clerk, *Phys. Rev. X* **5**, 021025 (2015).
- [13] L. D. Tóth, et al., arXiv:1602.05180, (2016).
- [14] C. F. Ockeloen-Korppi, et al., arXiv:1602.05779 (2016), to appear in PRX.
- [15] T. C. Ralph, A. P. Lund, and A. Lvovsky, in *QCMC: Ninth International Conference on QCMC* (AIP, 2009), pp. 155–160.
- [16] P. Lähteenmäki, et al., *J. Low Temp. Phys.* **175**, 868 (2014).
- [17] C. Gardiner and M. J. Collett, *Phys. Rev. A* **31**, 3761 (1985).
- [18] Note1, the subscript  $\omega$  stands for the frequency, and we use the Fourier convention where  $a_{\omega}^{\dagger}$  is the conjugate of  $a_{\omega}$ .
- [19] D. F. Walls and G. J. Milburn, *Quantum optics* (Springer Berlin Heidelberg, 2008).
- [20] M. Aspelmeyer, T. J. Kippenberg, and F. Marquardt, *Rev. Mod. Phys.* **86**, 1391 (2014).
- [21] C. M. Caves, et al., *Rev. Mod. Phys.* **52**, 341 (1980).
- [22] V. B. Braginsky, Y. I. Vorontsov, and K. S. Thorne, *Science* **209**, 547 (1980).
- [23] A. A. Clerk, F. Marquardt, and K. Jacobs, *New J Phys* **10**, 095010 (2008).
- [24] J. B. Hertzberg, et al., *Nat. Phys.* **6**, 213 (2009).
- [25] E. E. Wollman, et al., *Science* **349**, 952 (2015).
- [26] J. M. Pirkkalainen, et al., *Phys. Rev. Lett.* **115**, 243601 (2015).
- [27] F. Lecocq, et al., *Phys. Rev. X* **5**, 041037 (2015).